

Determination of Effective Permeability with Micro-Modeling of Digitized Core Images

Amir H. Hosseini, Oy Leuangthong and Clayton V. Deutsch

Presence of short-scale variability in sand/shale sequences, preferential sampling of core data, and uncertainty in upscaling parameters are complications that make the inference of a reliable porosity – permeability relationship impossible. A simple yet effective way of overcoming these complications is micro-modeling. The central idea in micro-modeling is to use an additional source of information, namely digitized core images, to quantify the uncertainty in power-law averaging parameters and construct the porosity-permeability bivariate relationship by Monte Carlo Simulations (MCS). The work-flow in micro-modeling is comprised of a few steps from digitizing the selected core images to building 3D geo-blocks of binary sand/shale mixture, populating them with porosity/permeability values, upscaling the populated binary mixture by flow simulations, determining the uncertainty in power-law parameters and implementing MCS. The porosity-permeability relationships are constructed on a by-facies basis. Results of this research suggest that effective properties of clean sand are changing with the volume fraction of shale; and it has ultimately resulted in the development of an extended version of power-law formalism.

Background

Mini-modeling technique (McLennan et al. 2006) was developed to (1) mitigate the bias in core porosity and permeability measurements, (2) infer bivariate relationship between porosity and permeability with limited core data and (3) account for the difference between the scales of core data and geological modeling grid blocks. However, there are a number of shortcomings associated with mini-modeling: implementation of mini-modeling still requires a number of representative parameters at the core-scale; it ignores the effect of laminae on core permeability measurements; and it neglects the uncertainty in the upscaling parameters.

Micro-modeling through the use of digitized core images has been recently developed to investigate the uncertainty in upscaling parameters in different scales, to account for important micro-scale features with high permeability contrasts, to account for preferentially sampled porosity and permeability data, and finally to support the establishment of representative statistics for mini-modeling. A direct result of micro-modeling is by-facies porosity-permeability relationship that would support the reservoir modeling at scales larger than core plug scale.

Digitized core images carry important information about micro-scale features and laminae which have profound impact on the fluid flow and are often dismissed in core data sampling efforts. High-resolution core photographs usually have pixel sizes equal to or smaller than a millimeter. The photographs used in this work have pixel sizes of 500 μm on each side. The overall workflow in micro-modeling includes selecting and digitizing by-facies core-photos, creating 3D training images (TIs) from the 2D data sets, creating 3D geo-blocks of sand/shale binary mixture, populating the binary mixture with appropriate porosity and permeability values, upscaling them to core-plug size, finding the distribution of upscaling parameters and performing MCS to find the representative porosity-permeability relationship on a by facies basis. The details of the proposed methodology are discussed in the following paragraphs.

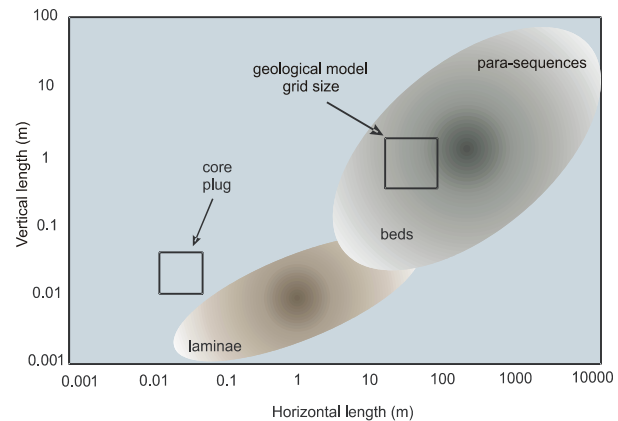


Figure-1: Core-plug size and geological modeling grid size in comparison to multi-scale heterogeneities

Construction of binary mixture geo-blocks

The first step in micro-modeling is the selection of core images on a by-facies basis (Figure 2). The black intervals in the core photos are coded as sand and the grey intervals are coded as shale. In the context of this work, it has been presumed that different facies are recognized due to different configuration and geometry of sand-shale sequences. Laminated sequences are assigned a facies type of Sandy or Muddy Inclined Heterolithic Strata (SIHS or MIHS) depending on the fraction of shale; and brecciated sequences are identified as the facies Breccia. After selection of and digitizing the images, the preliminary statistics such as histogram and indicator variograms are calculated for the 2D TIs.

A real challenge in micro-modeling is to extract 3D training images from the 2D digitized images. This problem has been partially addressed in the context of reconstruction of particulate media and micro-structures. In similar works, Roberts (1997) and Talukdar et al. (2002) proposed statistical methodologies in which the reconstructed 3D models share two-point correlation and chord distribution function with the original composite. More recently, Okabe and Blunt (2005) used Multiple Point Statistics (MPS) to generate 3D pore space representations from 2D thin sections as TIs. They used multiple template sizes and multigrid simulation, and concluded that the use of MPS gives a better prediction of long-range connectivity structures than the standard two-point statistics approaches.

In all of the above-mentioned works hypothesis of isotropic medium was presumed, which is irrelevant in the case of micro-modeling. Assuming the medium is isotropic in horizontal direction, a simple mirror imaging of the 2D TIs was applied. Three configurations were assumed for the TIs depending on the number of times mirror imaging was implemented and orientation of datasets relative to the target 3D geo-block (Figure 3). Application of each of these 3D datasets depends on the facies being modeled and checked by variogram reproduction. A certain area of future research is using MPS and theory of runs (chord statistics) in reconstructing the 3D TIs from the 2D core photos.

Using the mirror imaged 3D dataset, geo-blocks are then populated by a binary mixture of clean sand / shale by SISIM (Deutsch and Journel 1998). Figure 4 shows the geo-blocks of the binary mixture for the three different datasets. As mentioned previously, reproduction of two-point correlation structure and visual calibration to the 2D image can be used to choose the appropriate configuration of mirrored dataset and associated binary mixture geo-block. Configuration (c) often shows a better variogram reproduction for laminated facies and configuration (a) delivers better results for brecciated facies.

After construction of 3D geo-blocks of binary mixture of clean sand and shale at nominal micro-scale, appropriate distribution of porosity and permeability values must be assigned. There are a number of assumptions to this: (1) the porosity and permeability of shale are very small constant values; (2) At very small scale, porosity and log horizontal permeability of sand are spatially correlated and have Gaussian distributions; and (3) at very small scale, porosity and log horizontal permeability of sand are uncorrelated to each other. Based on these assumptions, mean and standard deviation of porosity and log permeability of clean sand are sufficient for the modeling purposes and should be independently calculated.

Mixture-modeling approaches from simple probability-plot regression to more advanced expectation-maximization and Markov-chain Monte Carlo approaches can be sought for this purpose. In mixture-modeling, it is assumed that each of distributions of porosity and horizontal permeability of sand facies is a mixture of two underlying Gaussian distributions, one representing clean sand. In the context of probability-plot regression approach, these two Gaussian distributions can be detected by fitting two straight lines on the probability plot (Figures 5, 6) of sand facies porosity or horizontal permeability. The strength of mixture modeling approaches is in their simplicity and independence of V_{shale} distribution which is not available in core plug scale. An alternative approach can be considered for the cases where V_{shale} has the same support as the available data (e.g. full-diameter core data); that is histogram matching (Figure 7). In histogram matching, mean and standard deviation of clean sand are calibrated by matching the simulated histograms of sand facies porosity and permeability with the observed counterparts. In addition to porosity and horizontal permeability, vertical to horizontal permeability ratio must also be determined. This can be done by repeating the calibration procedure for vertical permeability and finding the ratio of the means. The standard deviation of K_v/K_h is simply obtained from the original dataset for the sand facies. After calibration of the mean and standard deviation of porosity, horizontal permeability and

K_v/K_h ratio of clean sand, the geo-blocks comprising of clean sand – shale binary mixture are populated with the calibrated distributions using sequential Gaussian simulations (SGS). An example realization is presented in Figure 8.

Flow simulation and upscaling

Effective permeability can be written as power-law average of constituent permeabilities, that is:

$$K_{eff} = \left[\sum_{i=1}^{n_c} p_i k_i^\omega \right]^{\frac{1}{\omega}} \quad [1]$$

For a binary mixture, equation (1) can be rewritten as:

$$K_{eff} = \left[V_{SH} K_{shale}^\omega + (1 - V_{SH}) K_{sand}^\omega \right]^{\frac{1}{\omega}} \quad [2]$$

where, ω is power law averaging exponent, V_{SH} is V_{shale} attribute, and K_{shale} and K_{sand} are constituent permeabilities for shale and clean sand, respectively. The power law averaging exponent ω and percolation threshold P_c are central to power-law averaging in upscaling applications (Figure 9).

It is well-grounded in theory that the power law averaging exponent ω depends solely on the geometry of the sand-shale mixture, flow direction and percolation threshold (Deutsch 1989 among others). In other words, ω is independent of constituent permeabilities and sand-shale proportions in the mixture. The power law averaging exponent varies between -1.0 (harmonic average) and 1.0 (arithmetic average) and it is often estimated by performing flow simulations.

In this context, percolation threshold P_c is closely related to invasion percolation concepts and represents the critical V_{shale} value at which there is a significant change in the flow regime in the system, that is, dominant contribution of low-permeability material (shale) in fluid flow through the heterogeneous porous medium. As shown in Figure 9, power-law averaging exponent ω takes considerably different values below and above percolation threshold.

The percolation threshold (P_c), power law averaging exponent below P_c (ω_b), and power law averaging exponent above P_c (ω_a) are facies dependent and have uncertainty. To investigate the uncertainty in these parameters on a by-facies basis, flow simulation is performed on an ensemble of micro-models. Multiple core images are selected for laminated and brecciated facies and corresponding micro-models (multiple realizations) are constructed using the approach described earlier. Flow simulation is used to upscale the petrophysical properties from nominal micro scale ($500 \mu\text{m} \times 500 \mu\text{m} \times 500 \mu\text{m}$) to nominal core plug scale ($2.5 \text{ cm} \times 2.5 \text{ cm} \times 2.5 \text{ cm}$). The results of flow simulations in form of porosity – permeability and V_{shale} – permeability bivariate relationship is presented in Figures 10 and 11. Large uncertainties are observed in the value of percolation threshold and power law averaging exponents for vertical flow direction (K_v) for the laminated facies. These uncertainties are relatively smaller for the brecciated facies.

Statistical distribution of upscaling parameters can be obtained by fitting P_c , ω_b and ω_a for different ensembles of realizations constructed for different core images of the same facies type.

MCS with uncertain upscaling parameters

According to equations [1] and [2], an analytical model for effective permeability can be parameterized in terms of:

- Sand permeability at the smallest scale;
- $K_v:K_h$ ratio at the smallest scale;
- Shale permeability at the smallest scale;

- Horizontal and vertical percolation threshold; and
- Power law averaging exponents – below and above P_c .

A GSLIB-like program MCS_binmixture was prepared based on the above parameterization. Using the analytical solution and the associated program for Monte Carlo simulations, by-facies $\phi - K_h - K_v$ relationships can be obtained (Figure 12).

```

MCS for Effective Permeability
*****

START OF PARAMETERS
perm.out          -output file
10000             -number of realizations
02102008         -random number seed
0.20 0.40        -Vsh: mean (fraction), standard deviation
0.33 0.02        -Porosity sand: mean (fraction), standard deviation
3000.0 0.5       -K sand: median (mD), standard deviation (log10)
3000.0           -K sand at shale content of 0.25 (25%)
1.0 10000.0     - minimum (mD), maximum (mD)
0.90 0.1        -KV/KH: mean, standard deviation
0.75 1.0        - minimum, maximum
1.0 1.0         -K shale: median (mD), standard deviation (log10)
0.001 10.0     - minimum (mD), maximum (mD)
0.85 0.05      -Horizontal Percolation threshold, standard deviation
0.55 0.05      -Vertical Percolation threshold, standard deviation
0.60 0.05      -Horizontal exponent below Pc: mean, std dev
-0.20 0.05     -Horizontal exponent above Pc: mean, std dev
0.50 0.05      -Vertical exponent below Pc: mean, std dev
-0.40 0.05     -Vertical exponent above Pc: mean, std dev

```

Parameter file for MCS_binmixture program

Extended power law formalism (EPLF)

As mentioned previously, the effective permeability can be written as a power law average of the volume fraction of shale, the permeability of shale and the permeability of sand (equation [2]). Flow simulation indicates that the averaging exponent is largely independent of the volume fraction of shale and the constituent permeabilities; it depends on the geometry of the sand-shale. This model has been validated by flow simulation (Journal et al. 1986, Deutsch 1989). The results of the associated MCS, however, are not in full agreement with practical data; the permeability values for intermediate porosity values appear too high (Figure 13-a), as compared to experimental data.

The main reason for the too high permeability for intermediate porosity values is that the properties of the sand depend on the amount of shale. As the volume fraction of macroscopic shale increases, there are more small scale variations in sand. The porosity may not be affected significantly, but the sand permeability is reduced as V_{SH} increases (Porosity decreases). There are many reasons for this. The main reason is the reduced energy of deposition relative to thicker clean intervals of sand. The lower energy of deposition leads to poor sorting, reduced grain size, and presence of microscopic shales/clays. The result is lower permeability.

A log-linear decrease in the average permeability of clean sand with an increase in V_{SH} appears reasonable given experimental data. Figure 13-b shows the sand permeability (all samples flagged as clean sand) relative to the macroscopic collocated V_{SH} from well logs. A mathematical model for how the average sand permeability reduces with V_{SH} can be written as a function of the clean sand permeability and the sand permeability at an arbitrary macroscopic shale volume:

$$\log(\overline{K}_{sand}(V_{SH})) = \log(\overline{K}_{clean\ sand}) - \frac{V_{SH}}{0.25} \left[\log(\overline{K}_{clean\ sand}) - \log(\overline{K}_{0.25}) \right] \quad [3]$$

where, $\overline{K}_{sand}(V_{SH})$ is the average reduced sand permeability for a given V_{SH} , $\overline{K}_{clean\ sand}$ is the average clean sand permeability obtained from mixture modeling with sand facies, and $\overline{K}_{0.25}$ is the reduced sand permeability at a V_{SH} value of 0.25, and must be fitted by comparing to experimental data. The results appear promising and able to fit experimental data. Figure 14 shows the effect of various fitted $\overline{K}_{0.25}$ values on porosity – horizontal permeability relationship. The model is flexible and grounded in physics; however, a criticism is that there are too many parameters to fit. There is only one additional parameter and the results should no be over-fit. The calibration of $\overline{K}_{0.25}$ should be conducted using the facies with the largest dataset.

In order to validate the proposed methodology, a flow simulation study was carried out. For this purpose, the flow simulator code (flowsim) was modified to account for the changes in properties of sand with changes in macroscopic shale content (flowsim_eplf).

```

                                FLOWSIM PARAMETERS
                                *****

START OF PARAMETERS:
perm-12-1.out                    -file with original dataset
2 3 4 0 0 5 1                    - columns for kx,ky,kz,ky/kx,kz/kx,phi,vshale
6120.0                            -Clean sand: Mean kh
0.204                             - Standard deviation(log10)
0.93                               - kv:kh
400.0                              -kh sand at %25 shale content
flowsim.out                       -output file for effective properties
153 153 280                       -input: nx,ny,nz
1.0 1.0 1.0                       -input: dx,dy,dz
3 3 5                              -output: nx,ny,nz

```

Parameter file for flowsim_eplf program

Figure 15 shows the results of the validation study, in which porosity – vertical permeability bivariate relationship for a micro-model from Monte Carlo Simulations is compared to corresponding flow simulation results. A $\overline{K}_{0.25}$ equal to 400 mD has been used in the study.

Application of micro-modeling and EPLF

In the previous sections, a micro-modeling approach was proposed to account for sampling bias and to construct the bivariate porosity-permeability relationship in presence of sparse data. To show the application of the proposed methodology for McMurray Oilsands, a number of core photos have been selected, digitized and used in generating multiple micro-modeling realizations for laminated and brecciated facies (SIHS, MIHS and Breccia). The extended power law formalism (EPLF) with $\overline{K}_{0.25}$ equal to 400 mD was used and bivariate relationship between porosity and permeability was build for different facies. Figures 16, 17 and 18 compare the simulated and observed porosity-vertical permeability cross-plots for SIHS, MIHS, and Breccia facies, respectively.

Conclusions

A micro-modeling approach was proposed to account for (1) sampling bias, (2) small laminated features with high permeability contrast, and (3) uncertainty in upscaling parameters. In line with micro-modeling, the extended power-law formalism was also proposed to account for changes in clean sand permeability as a function of macroscopic shale content. The proposed mathematical model was tested against flow simulation results and a close agreement was observed. The proposed methodology was also applied to build the porosity – permeability relationship for laminated and brecciated facies of McMurray oilsands and a good agreement with the experimental data was observed.

References

- Deutsch, C.V., 1989, Calculating Effective Absolute Permeability in Sandstone/Shale Sequences. *SPE Formation Evaluation Journal*, 4(3): 343-348. SPE Paper 17264.
- Deutsch, C.V. and Journel, A.G., 1998, *GSLIB: Geostatistical Software Library: and User's Guide*, Oxford University Press, New York, 2nd Ed.
- Journel, A.G., Deutsch, C.V., and Desbarats, A.J., 1986. Power-Averaging for Block Effective Permeability. *SPE California Regional Meeting*, 2-4 April 1986, Oakland, California, SPE Paper 15991.
- McLennan, J.A., Deutsch, C.V., Wheeler, T.J., Richey, J.F. and Mus, E., 2006, SAGD Permeability Modeling using Geostatistics and Mini-Models. *SPE Annual Technical Conference and Exhibition*, 24-27 September 2006, San Antonio, Texas, SPE Paper 103083.
- Okabe, H., Blunt, M.J., 2005, Pore space reconstruction using multiple-point statistics. *Journal of Petroleum Science and Engineering*, 46: 121 – 137.
- Roberts, A.P., 1997, Statistical reconstruction of three-dimensional porous media from two-dimensional images. *Physical Review E*, 56(3).
- Talukdar, M.S., Torsaeter, O. and Ioannidis, M.A., 2002, Stochastic Reconstruction of Particulate Media from Two-Dimensional Images. *Journal of Colloid and Interface Science*, 248: 419 – 428.

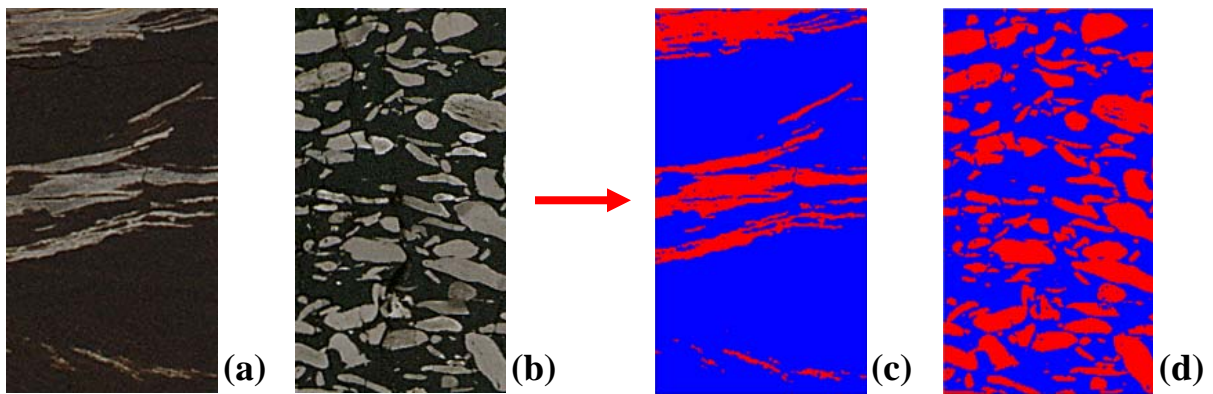


Figure-2: Two selected core photos representing laminated (a) and brecciated (b) facies types and their corresponding digitized images (c) and (d).

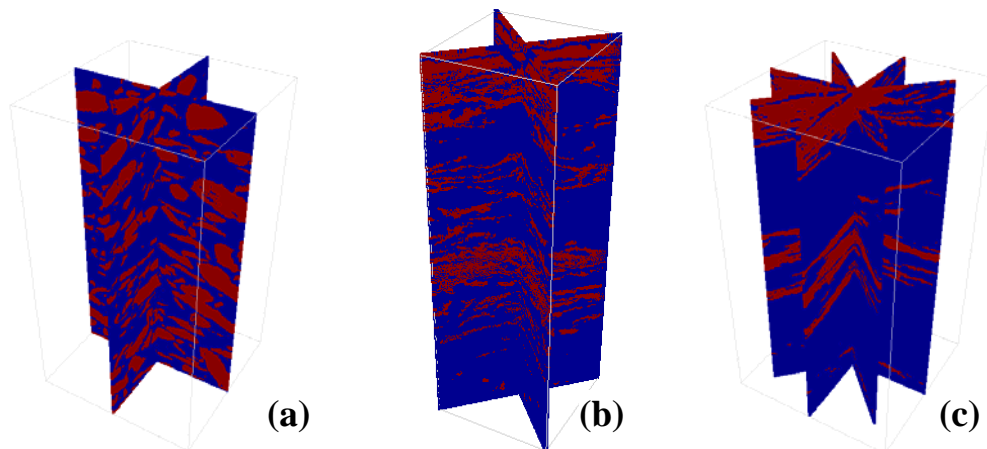


Figure-3: Three different configurations for the 3D dataset to be used in constructing the 3D geo-block (training image)

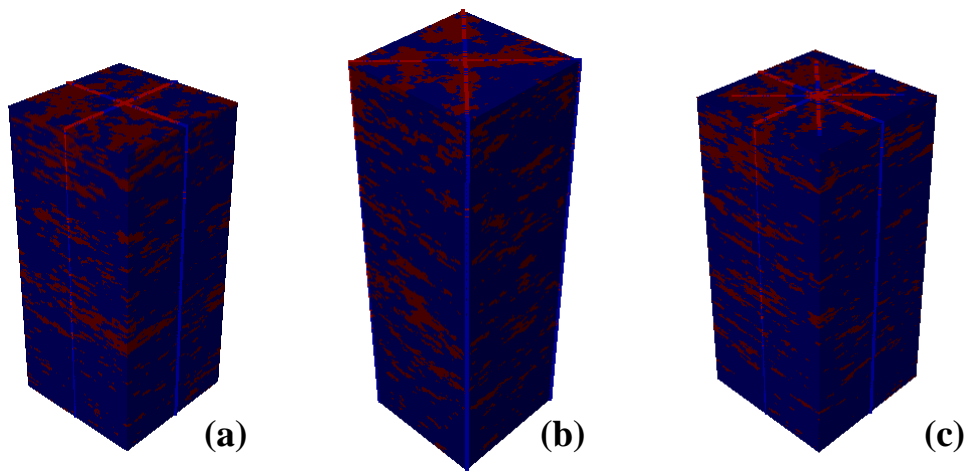


Figure-4: The geo-blocks of clean sand – shale binary mixture for different mirrored data configurations

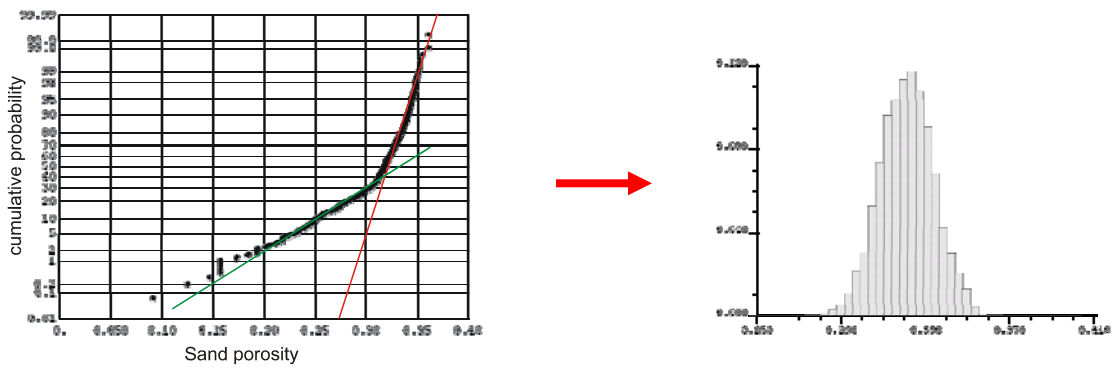


Figure-5: Probability-plot regression for clean sand porosity

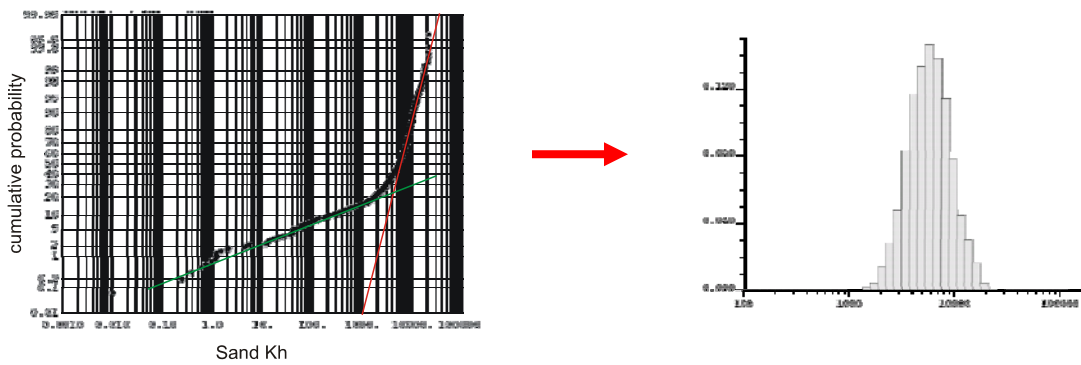


Figure-6: Probability-plot regression for clean sand horizontal permeability

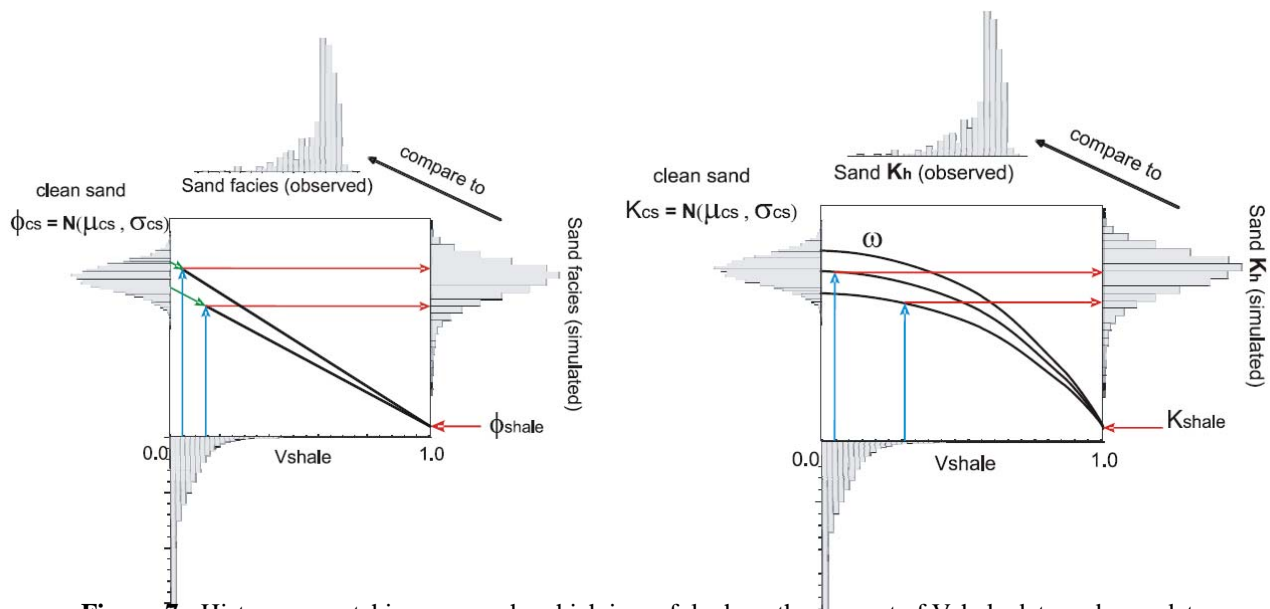


Figure-7: Histogram matching approach, which is useful where the support of Vshale data and core data are comparable (e.g. full-diameter core).

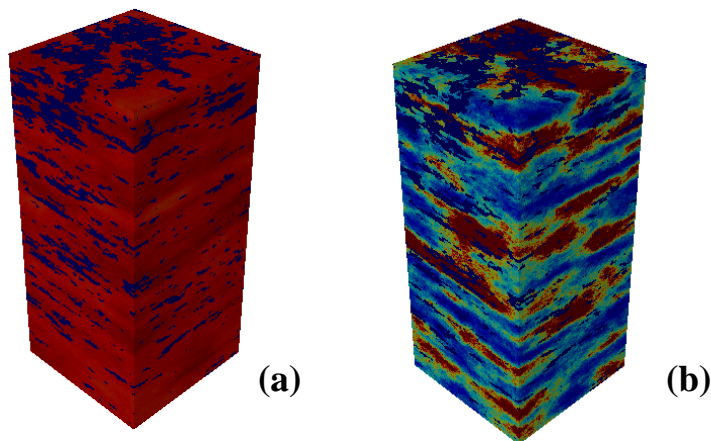


Figure-8: A representative geo-block populated by calibrated clean sand / shale properties

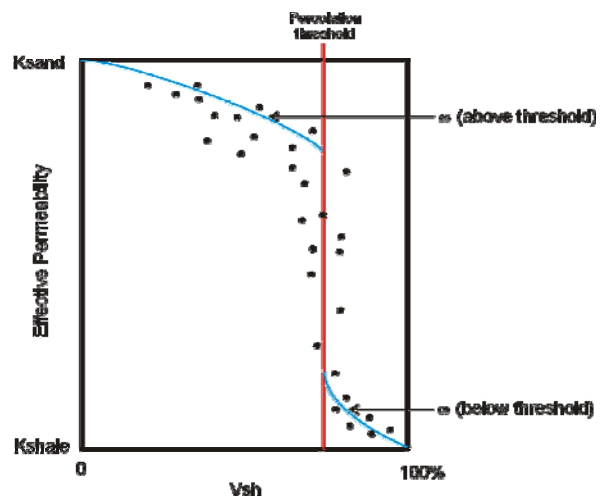


Figure-9: Variations of effective permeability as a function of V_{SH} . Power law averaging exponent changes at percolation threshold.

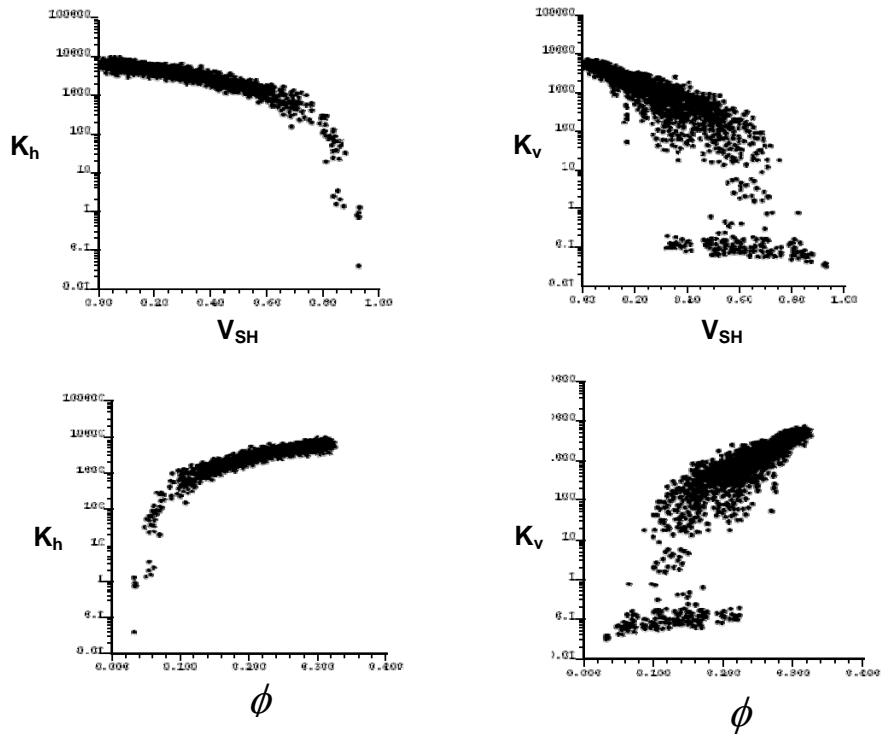


Figure-10: Porosity-permeability and Vshale-permeability relationships obtained by upscaling to core-plug scale for laminated facies (e.g. SIHS).

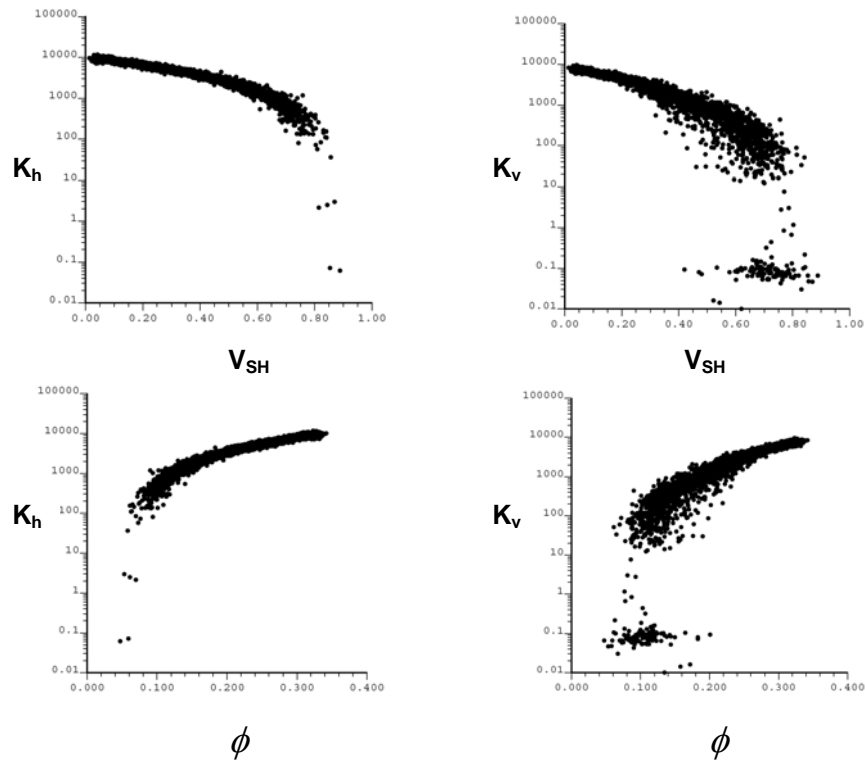


Figure-11: Porosity-permeability and Vshale-permeability relationships obtained by upscaling to core-plug scale for brecciated facies (e.g. Breccia).

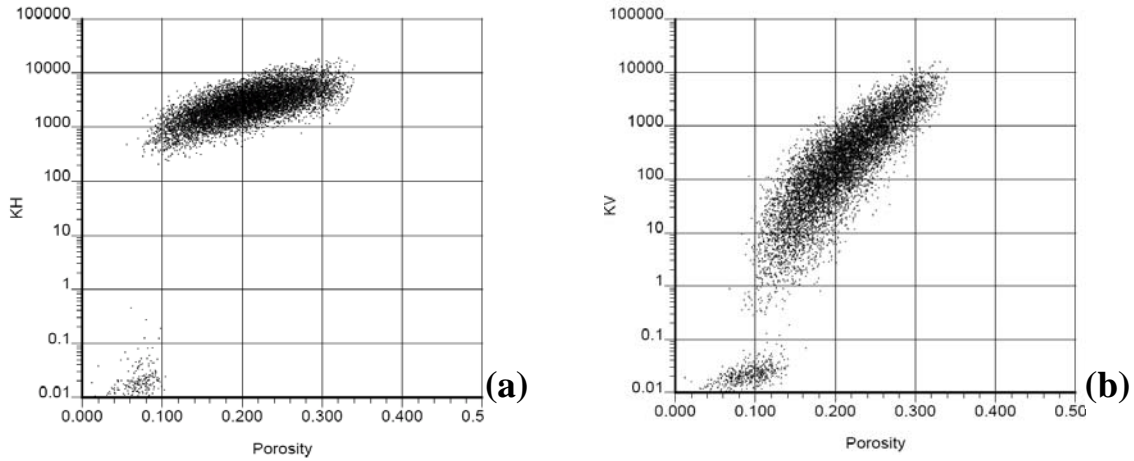


Figure-12: Porosity-permeability relationships for horizontal (a) and vertical (b) permeabilities resulted from Monte Carlo Simulations

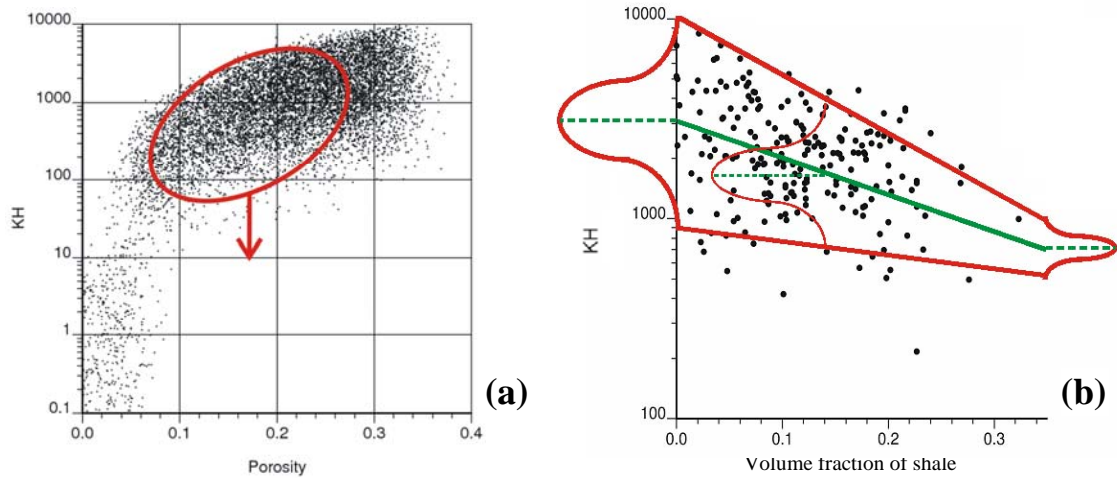


Figure-13: The permeability values resulted from the MCS appear too high for intermediate porosity values (a); log-linear relationship between the permeability of clean sand and volume fraction of shale (b).

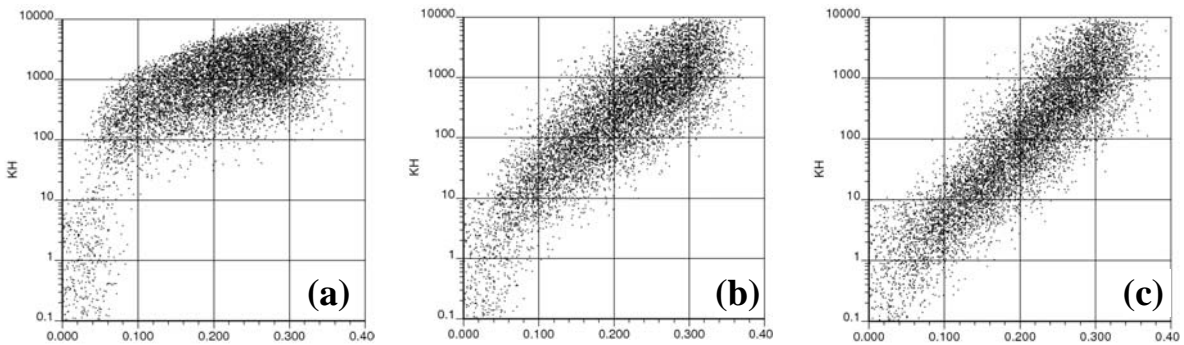


Figure-14: Porosity-permeability relationships for (a) $\bar{K}_{0.25}=3000$, (b) $\bar{K}_{0.25}=1000$, (c) $\bar{K}_{0.25}=500$.

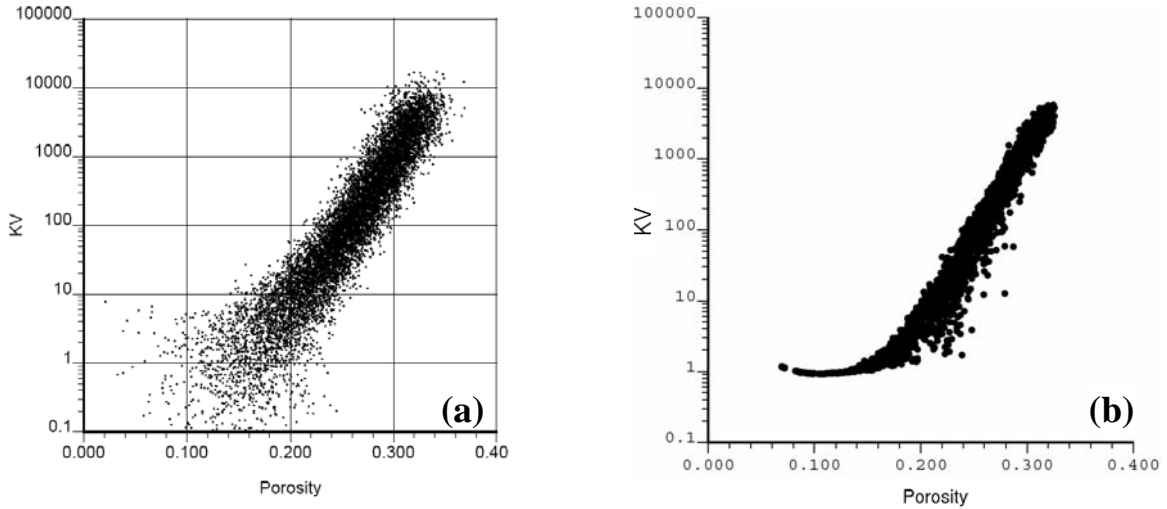


Figure-15: Validation of extended power law formalism by flow simulation: Monte Carlo Simulation results (a), corresponding flow simulation results (b).

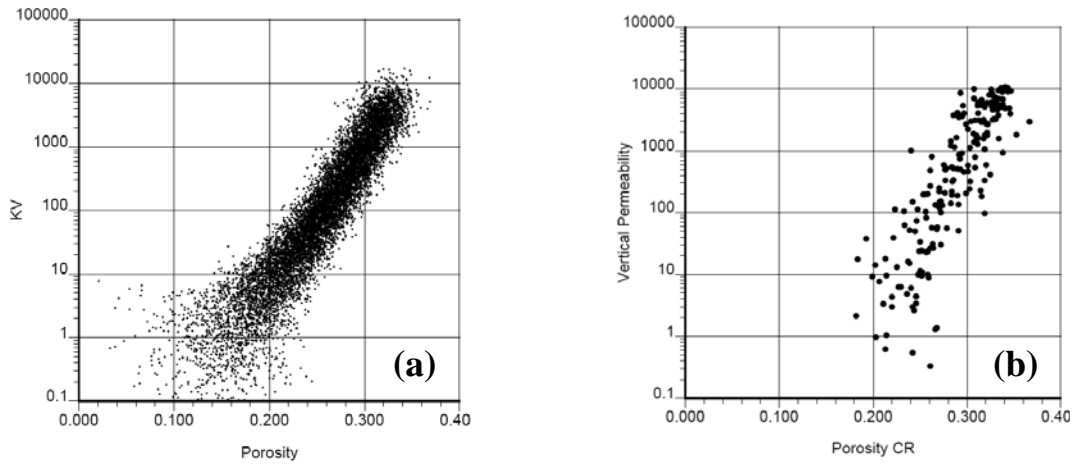


Figure-16: Simulated (a) versus observed (b) bivariate $\phi - K_v$ relationship for SIHS facies.

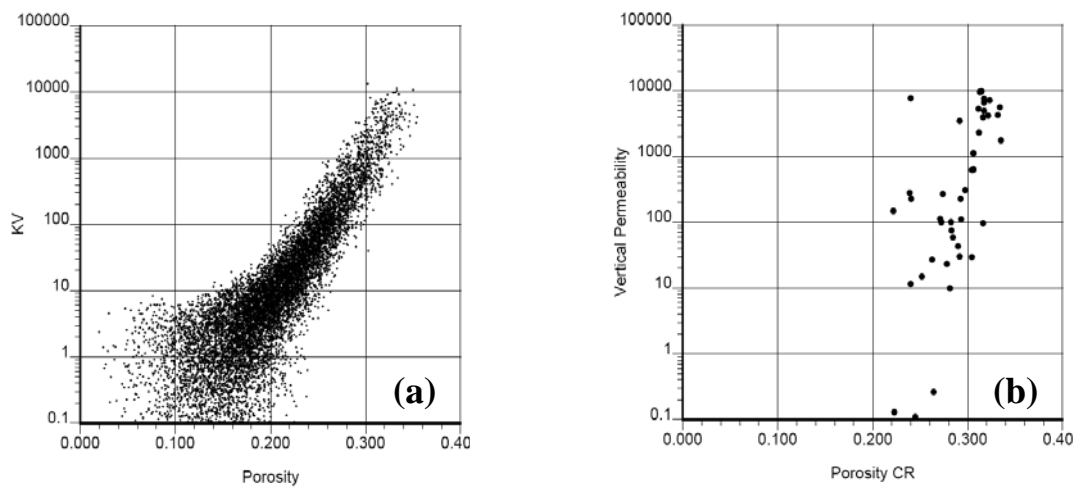


Figure-17: Simulated (a) versus observed (b) bivariate $\phi - K_v$ relationship for MIHS facies.

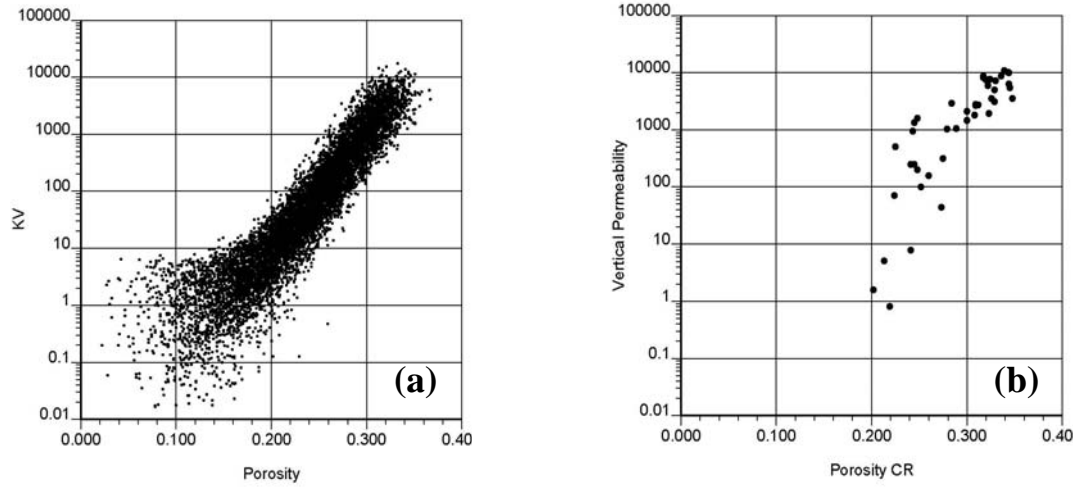


Figure-18: Simulated (a) versus observed (b) bivariate $\phi - K_v$ relationship for Breccia facies.